Sep. 2013, Volume 7, No. 9 (Serial No. 70), pp. 1111-1117
Journal of Civil Engineering and Architecture, ISSN 1934-7359, USA

Changes in Coupled Vibration Frequencies and Modes of Wall-Cavity Systems Induced by Stiffness Variation in the Structure

Soraya Mendes de Souza[1], Lineu José Pedroso[1] and Paulo Marcelo Vieira Ribeiro[2]

1. College of Technology, University of Brasilia, Brasilia 70904-108, Brazil

2. Civil Engineering Department, University of Pernambuco, Recife 50740-530, Brazil

Abstract: Problems of fluid structure interactions are governed by a set of fundamental parameters. This work aims at showing through simple examples the changes in natural vibration frequencies and mode shapes for wall-cavity systems when the structural rigidity is modified. Numerical results are constructed using ANSYS software with triangular finite elements for both the fluid (2D acoustic elements) and the solid (plane stress) domains. These former results are compared to proposed analytical expressions, showing an alternative benchmark tool for the analyst. Very rigid wall structures imply in frequencies and mode shapes almost identical to those achieved for an acoustic cavity with Neumann boundary condition at the interface. In this case, the wall behaves as rigid and fluid-structure system mode shapes are similar to those achieved for the uncoupled reservoir case.

Key words: Fluid-structure, finite element, vibration modes, acoustic cavities.

Nomenclature

Abbreviations

AM	Additional mass mode shape
DS	Structural dominant mode shape
DS/AM	Mixed mode shape, with structural dominant and added mass characteristics
FW	Coupled one dimensional flat wave mode shape
DC	Acoustic cavity dominant mode shape
AR	Additional rigidity mode shape
DC/AR	Mixed mode shape, with cavity dominant and added rigidity characteristics
closed	Cavity with Dirichlet boundary prescribed at a given direction (rigid wall)

Symbols

x	Transverse direction
y	Longitudinal direction
p	Acoustic fluid pressure
ρ	Fluid density
u	Structural displacement
c	Sound velocity at fluid domain
g	Gravitational acceleration
Γ	Contour domain
$\vec{n}$	Vector normal to contour domain
$\hat{u}$	Structural displacement approximate solution
$\hat{p}$	Fluid pressure approximate solution
$\bar{u}$	Structural displacement nodal variables vector
$\bar{p}$	Fluid pressure nodal variables vector
$\{L\}$	Derivative vector
$\nabla p \approx \nabla \hat{p}$	Pressure derivative
$[Np]$	Shape factor matrix related to fluid pressures
$[Nu]$	Shape factor matrix related to structural displacements

Corresponding author: Paulo Marcelo Vieira Ribeiro, D.Sc., research fields: structural dynamics, fluid-structure interaction, numerical methods and applied mathematics, reinforced concrete structures. E-mail: paulo.vribeiro@ufpe.br.

1. Introduction

Coupled problems related to fluid-structure interactions can be found in various branches of engineering. The studies of these problems appear in several cases of cavities containing fluid and it is associated to structures that can be elastic, flexible/rigid, as well as in pipes and ducts with fluid on the outside/inside, and so on. Since this is a multi-physic problem, elements of the global matrix are represented by physical and geometrical constant of the involved domains, which have very different magnitudes, that complicates the resolution of these systems. Therefore, a segment of the literature is dedicated to the study of simplified models.

The current formulation considers an acoustic fluid (without flow), which simplifies the model. The movements are small around an equilibrium position, where there are only pressure waves. Among the classic formulations that deal with coupled fluid-structure problems are: (1) the Lagrangian, which has been used, for example, by Zienkiewicz and Bettess [1] and Wilson and Khalvati [2], among others; (2) the Eulerian, which has been characterized by the pressure, a displacement or velocity potential for the fluid, and the displacement as a variable for the solid, such as described by Zienkiewicz and Newton [3] and others [4-7].

Considering the numerical disadvantages related to unsymmetrical systems, Everstine [5] proposed a formulation based on velocity potential to solve this problem. Olson and Bathe [8] introduced hydrostatic pressures on the formulation and made it possible to deal also with static problems. This method was also used by Galli and Pavanello [9] among others [10-13].

This work uses simple test cases, which can be compared to analytical solutions, to show the application of the potential formulation (U-P), as described by Sousa [14] implemented in ANSYS [15]. Numerical results obtained with this software are compared to an equivalent analytical solution. Finite element models are constructed with simple triangular elements of the plane stress state, as well as triangular elements with linear interpolation functions for the fluid.

The proposed development is organized in three main categories: (1) theoretical formulation, with the multi-physic problem governing equations; (2) analyses results, along with numerical and analytical solutions, as well as comparison and discussion over results; (3) conclusions with final comments.

2. Theoretical Formulation

Application of the Galerkin method to the wave equation provides, as shown by Everstine [5], Souza [13] and Sousa [14]:

$$-\int_{\Omega_f} \nabla\hat{p}\cdot\nabla\hat{p}\cdot d\Omega_f - \oint_{\Gamma 1} \rho\cdot\ddot{\mathrm{u}}\cdot\vec{\mathrm{n}}\cdot\hat{p}\cdot d\Gamma_1 - \oint_{\Gamma 3}\frac{1}{c}\cdot\dot{\hat{p}}\cdot\hat{p}\cdot d\Gamma_4 - \oint_{\Gamma 4}\frac{1}{g}\cdot\ddot{\hat{p}}\cdot\hat{p}\cdot d\Gamma_3 - \int_{\Omega_f}\frac{1}{c^2}\cdot\ddot{\hat{p}}\cdot\hat{p}\cdot d\Omega_f = 0 \quad (1)$$

where, $\vec{n}$ is a vector in the normal direction to the boundary, where there is interaction with structure. As the problem is discretized by finite elements, the authors have the pressure $\hat{p}$ approximated by:

$$p \approx \hat{p} = [Np]\cdot\{\overline{p}\},\quad \nabla p \approx \nabla\hat{p} = \nabla[Np]\cdot\{\overline{p}\} = \{L\}\cdot[Np]\cdot\{\overline{p}\} = [Bp]\cdot\{\overline{p}\} \quad (2)$$

where, $\{L\} = \{\partial/\partial X \quad \partial/\partial Y\}^T$.

By applying the discretized form of the variables in Eq. (1), the problem is transformed to the following matricial equation (equation of fluid motion, as shown by [5, 13, 14]):

$$[K_f]\cdot\{\overline{p}\}+[M_f]\cdot\{\ddot{\overline{p}}\}+\rho\cdot[FS]^T\cdot\{\ddot{\overline{u}}\}+[SL]\cdot\{\ddot{\overline{p}}\}+[R]\cdot\{\dot{\overline{p}}\}=0 \quad (3)$$

where:

$[K_f]$ = stiffness matrix of the fluid;

$[M_f]$ = mass matrix of the fluid;

$[FS]$ = fluid-structure coupled matrix;

$[R]$ = radiation condition matrix at infinity;

$[SL]$ = free surface matrix.

The coupled problem is solved simultaneously by the classical equations of motion of the structure Eq. (4) and the fluid Eq. (5).

In the structural equation of motion, the vector of forces $[FS]$ can be transformed into two vectors: a vector of forces (f) and a generic vector of force due to fluid pressure at the interface with the solid domain "[FS]. $\overline{p}$". Therefore, the equations of motion for the solid and fluid domains are [5, 13, 14]:

$$[M_E]\cdot\{\ddot{\overline{u}}\}+[C_E]\cdot\{\dot{\overline{u}}\}+[K_E]\cdot\{\overline{u}\}-[FS]\cdot\{\overline{p}\}=[f] \quad (4)$$

$$[M_f]\cdot\{\ddot{\overline{p}}\}+[SL]\cdot\{\ddot{\overline{p}}\}+[R]\cdot\{\dot{\overline{p}}\}+[K_f]\cdot\{\overline{p}\}+\rho\cdot[FS]^T\cdot\{\ddot{\overline{u}}\}=0 \quad (5)$$

The above equations can be arranged in a single matricial equation:

$$[M^*]\{\ddot{\delta}\} + [C^*]\{\dot{\delta}\} + [K^*]\{\delta\} = f^* \quad (6)$$

where, M^*, C^* and K^* are similar to mass, damping and stiffness matrices of an uncoupled system. The vector $\{\delta\}$ involves all degrees of freedom of the system (displacement and pressure).

Eq. (4) represents the most complete case of fluid-structure problem. However, to simplify the eigenvalue problem, matrix [C^*] can be eliminated which involves the structural damping and the radiation condition, as well as the free surface [SL], while transforming $f^* = 0$.

Moreover, in the case of natural vibrations, the displacements of the structure and fluid pressure vary along time, with a circular frequency ω. Thus, the authors can write the second derivate of function δ in time, i.e, $\ddot{\delta} = -\omega^2 \cdot \delta$. Then, Eq. (6) is given by: $([K^*] - \omega^2[M^*]).\{\delta\} = 0$.

This expression is the classical form of the eigenvalue and eigenvector problems. Solution of this latter equation provides the natural frequencies and the vibration modes of the system.

3. Results and Discussion

A test case is an open acoustic cavity, 1 m^2 × 1 m^2, with a rigid plate at the bottom, which is supported by an elastic spring (Fig. 1). It has rigid walls and the flexible base is modeled through a rigid plate with one vertical degree of freedom.

Material properties:

Solid domain:

$$t = 0.05\,m; \quad \nu = 0.3 \quad K = 80{,}000\ \frac{N}{m},$$

$$E = 2.1 \times 10^{11}\ \frac{N}{m^2};$$

Fluid domain:

$$\rho_s = 7{,}800\ \frac{kg}{m^3}; \quad \rho_f = 1{,}000\ \frac{kg}{m^3}; \quad \beta = 2.25 \times 10^9\ \frac{N}{m^2};$$

$$L = 1m\ ; \ c = 1{,}500\ m/s$$

3.1 Natural Frequencies and Vibration Modes for the Uncoupled Structure and Reservoir Using Proposed Analytical Expressions

The uncoupled natural modes of the structure were obtained analytically, and the numerical ones using ANSYS. The natural frequencies of the structure can be obtained by combining the dynamic behavior of the beam in bending condition and on an elastic base (springs) as show by Souza [13]:

$$f_i = \left(\frac{i^4 \pi^4}{4\pi^2 L^4} \frac{EI}{m} + \frac{k_f}{4\pi^2 \Delta m} \right)^{1/2} \quad (7)$$

where,

EI = bending stiffness;

m = mass per unit length of beam;

k_f = stiffness of elastic support per unit length of beam;

Δ = spacing between springs;

L = length of the beam.

In numerical solution, the solid mesh has 34 nodes with 16 triangular linear elements (plane stress state), arranged in a layer (Fig. 1a).

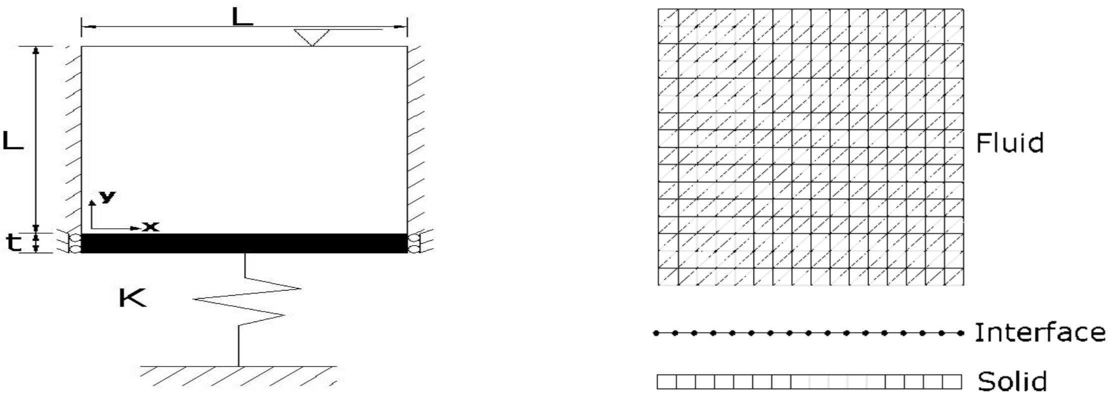

(a) (b)

Fig. 1 A test case: (a) open cavity with a rigid plate at the bottom; (b) mesh used in the discretization by FE of model.

The analytical natural frequency of the uncoupled cavity can be expressed as Ref. [13]:

$$\omega = \pi c\sqrt{\left(\frac{n_x}{L_x}\right)^2 + \left(\frac{n_y}{2L_y}\right)^2} \text{ and } p(x,y) = \cos\frac{n_x \pi x}{L_x}\cos\frac{n_y \pi x}{2L_y}$$
$$\Rightarrow n_x = 0,1,2,\ldots \text{ and } n_y = 1,3,5,\ldots \quad (8)$$

The vibration modes of the uncoupled cavity are obtained with the transfer matrix method as shown by Pedroso [10] and Souza [13], whose frequencies are given in Table 1.

3.2 Uncoupled System Numerical Solution Results and Comparison with Proposed Analytical Expressions

The mesh used in the discretization of the fluid domain has 512 elements (regular triangular elements), with a total of 289 nodes (Fig. 1b). Table 1 compares analytical and numerical results for the structure and uncoupled acoustic cavity.

The authors can observe that the zero mode (i = 0) is the "piston" mode with rigid body movement and constant deformed modal. Fig. 2 illustrates the first five typical modes of the uncoupled cavity and their natural frequencies.

3.3 Natural Frequencies and Vibrations Modes for the Coupled System Using Proposed Analytical Expressions

Analytical solution, Eq. (9) allows the calculation of natural frequencies of the coupled problem, as shown by Pedroso [10]:

$$\lambda^2\left(\mu + \frac{1}{\lambda} tg\, \lambda\right) = \alpha \quad (9)$$

where:

$\mu = \frac{m_s}{m_f} = \frac{m}{\rho_f SL} \Rightarrow$ ratio between structure and fluid masses;

$\alpha = \frac{K}{\frac{\rho_f c^2 S}{L}} = \frac{KL}{\beta S} \Rightarrow$ ratio between structure and fluid stiffnesses;

$\lambda = \omega L/c \Rightarrow$ compressibility parameter.

The coupled frequency is the combination of the uncoupled natural frequency in the x direction with the coupled frequency of the cavity, which can be expressed as follows [10]:

$$\omega = \sqrt{\omega^2_{uncoupled,x} + \omega^2_{coupled,y}} \quad (10)$$

Table 1 Analytical and numerical uncoupled frequencies for the structure and uncoupled acoustic cavity (rad/s).

Mode	Index	Uncoupled structure			Mode	n_x	n_y	Uncoupled fluid		
		Analytical with spring	Numerical with spring	Error (%)				Analitical Eq. (7)	Numerical ANSYS	Error (%)
1	i = 0	14.32	14.32	0.00	1	0	1	2,356.19	2,357.14	0.04
2	i = 1	739.29	740.16	0.12	2	1	1	5,268.61	5,282.53	0.26
3	i = 2	2,956.65	2,970.06	0.45	3	0	3	7,068.58	7,094.34	0.36
4	i = 3	6,652.40	6,721.12	1.03	4	1	3	8,495.38	8,558.33	0.74
5	i = 4	11,826.47	12,045.49	1.85	5	2	1	9,714.84	9,788.57	0.76

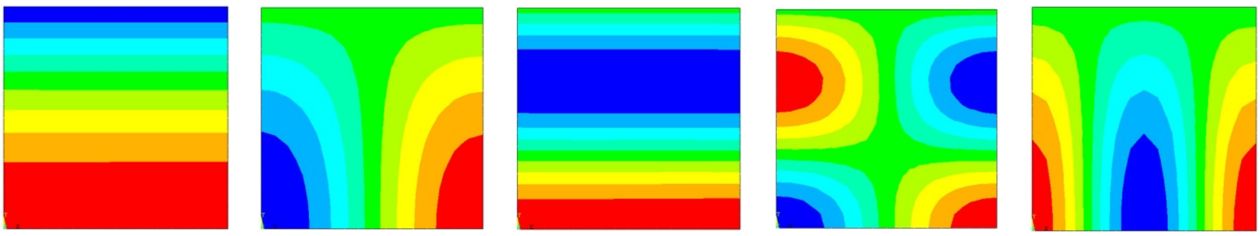

(a) Mode 1 2,357.14 rad/s (b) Mode 2 5,282.53 rad/s (c) Mode 3 7,094.34 rad/s (d) Mode 4 8,558.33 rad/s (e) Mode 5 9,788.57 rad/s

Fig. 2 Representation of uncoupled cavity vibration modes obtained with ANSYS.

Table 2 Coupled analytical frequencies for the wall-cavity system (rad/s).

n_y	n_x							
	0	1	2	3	4	5	6	7
1	7.59	-	-	-	-	-	-	-
2	3,586.65	5,922.05	10,084.17	14,585.05	19,187.75	23,833.37	28,500.91	33,181.14
3	7,758.90	9,077.84	12,207.66	16,126.38	20,383.97	24,806.57	29,319.59	33,886.94
4	12,237.80	13,113.70	15,446.33	18,698.18	22,473.72	26,550.48	30,809.10	35,183.61
5	16,830.40	17,477.63	19,289.57	21,980.00	25,269.88	28,955.59	32,904.39	37,032.21
6	21,471.60	21,982.65	23,449.03	25,707.78	28,571.60	31,877.82	35,503.08	39,359.30
7	26,137.30	26,558.70	27,784.61	29,715.61	32,225.20	35,189.82	38,504.49	42,086.60

Eq. (10) enables the construction of Table 2, in which the first line represents the uncoupled modes in the transverse direction (x) (n_x = 0, 1, 2, 3, ... 7). While the first column corresponds to the coupled modes in the longitudinal direction (vertical y) (n_y = 1, 2, 3, 4 ,..., 7) Therefore, to generate Table 2, the authors use the composition of the analytical frequencies in directions x and y.

The result of 7.59 rad/s is the typical frequency of added mass for $\lambda < 1$ (incompressible fluid). To generate the vibration modes of the cavity for the coupled problem, the authors can use the same reasoning. The authors develop the combination of the uncoupled vibration modes for a closed cavity in x direction with the coupled vibration modes for an open cavity in y direction. Thus, the authors get the modal form expression in both directions [10].

$$p(x,y) = \cos\left(\frac{n_x \pi x}{L_x}\right) . \left[-tg\,\lambda . \cos\left(\lambda \frac{y}{L}\right) + sen\left(\lambda \frac{y}{L}\right)\right] \quad (11)$$

3.4 Coupled System Numerical Solution Results and Comparison with Proposed Analytical Expressions

The discretization by finite elements of the coupled problem is presented below. Meshes of fluid and structural domains are the same as those adopted for the uncoupled case.

Figs. 3 and 4 correspond to the first five modes of the open coupled cavity with their natural frequencies, obtained with the ANSYS software using, respectively, $E = 2.1 \times 10^{11}$ N/m^2 and $E = 2.1 \times 10^{15}$ N/m^2.

Table 3 summarizes the results of the first five numerical and analytical frequencies for the coupled case, respectively, with modulus of elasticity $E = 2.1 \times 10^{11}$ N/m^2 (flexible structure) and $E = 2.1 \times 10^{15}$ N/m^2 (rigid structure). Moreover, it shows the differences in percentage between the analytically and numerically calculated values. These results present good agreement between them with small maximum errors (< 10%) for most of the frequencies analyzed in Table 3. Therefore, it is possible to predict the numerical results even for higher frequencies of the system from the coupled analytical solution, given by Eq. (10). Indeed, the analytical solutions are obtained by superposition of two independent 1-D solutions.

The columns indicated with * symbol was obtained with the inclusion of the additional mass (through the frequencies relation f_{water}/f_{vacum}), that was a result from coupled problem and then applied in the solution of the uncoupled beam.

It is noted that when the rigidity of the structure increases, only pure acoustic modes of the cavity arise, because the modes of the structure are eliminated in this range of frequencies, as shown in Fig. 4. Comparing the 2D representations in Fig. 4 with Fig. 2, the authors can see the similarity of the signature modes, with corresponding to sequence order.

The vibration modes of the coupled problem present a certain difficulty in the analysis and interpretation, as modes with typical characteristics of the structure, cavity and mixed (cavity + structure) appear, as shown in Fig. 3. In the analysis and interpretation of the modal shapes associated with the coupled fluid-structure problem, the following signature modal (default) is observed:

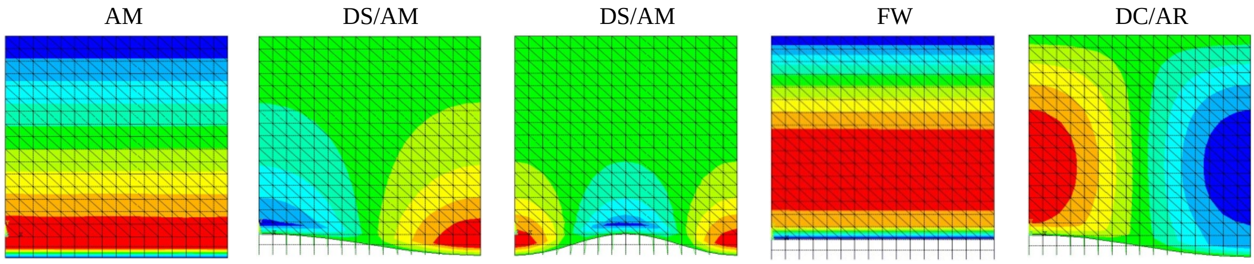

(a) Mode 1 7.28 rad/s | (b) Mode 2 550.28 rad/s | (c) Mode 3 2,506.30 rad/s | (d) Mode 4 3,590.02 rad/s | (e) Mode 5 5,944.02 rad/s

Fig. 3 Representation of coupled vibration modes obtained with ANSYS (E = 2.1 × 10^{11} N/m^2).

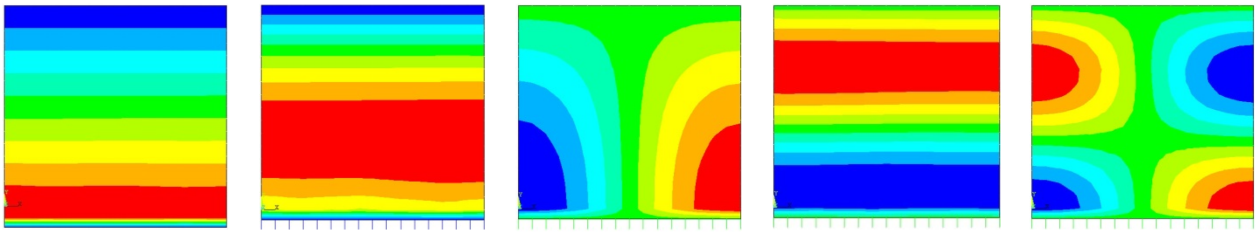

(a) Mode 1 7.28 rad/s | (b) Mode 2 3,586.63 rad/s | (c) Mode 3 5,277.18 rad/s | (d) Mode 4 7,803.09 rad/s | (e) Mode 5 8,550.16 rad/s

Fig. 4 Representation of coupled vibration modes obtained with ANSYS (E = 2.1 × 10^{15} N/m^2).

(1) Typical AM (additional mass) mode with lower frequency. In this case, the structure shows deformed rigid body movement (piston), a cavity with incompressible fluid and a ramp like mode;

(2) Structural dominant modes (typical deformed modes of the structure) with additional mass (DS/AM). The frequencies have values lower than the frequencies of the uncoupled structure. The fluid follows the structural deformed shape. There is no excitation of the cavity modes. When the fluid is disturbed, it acts as an additional mass on the structure;

(3) Dominant modes of the cavity with additional rigidity (DC/AR). Related to mode shapes of the uncoupled cavity with frequencies is higher than these cavity frequencies. The structure follows the pressure mode shapes of the cavity. The cavity behaves as if it acquired additional rigidity;

(4) Modes with FW (flat waves). It is characterized by strong coupling in the direction of the rigid body movement of the structure. The cavity reproduces the deformed 1D shape in the piston's direction in the order of its index (n_y). While in the transverse direction (x), the constant pressure mode always appear (n_x = 0), replicating the unidirectional shape mode of a

Table 3 Analytical and numerical coupled frequencies for the cavity with E = 2.1 × 10^{11} N/m^2 and E = 2.1 × 10^{15} N/m^2.

Mode index	Cav. mode		Str. mode	Frequencies with E = 2.1 × 10 E^{11}					Cav. mode		Frequencies with E = 2.1 × 10 E^{15}			
	n_x	n_y	n_i	Numerical coupled	Analytical coupled	Analytical coupled*	Dif.* (%)	Mode type*	n_x	n_y	Numerical coupled	Analytical coupled	Dif. (%)	Mode type
1	0	1*	0	7.29	7.59	7.59	3.95	AM	0	1	7.29	7.59	3.95	AM
2	-	-	1	550.28	739.29	549.38	0.16	DS/AM	0	2	3,586.63	3,586.65	0.00	FW
3	-	-	2	2,506.3	2,956.7	2,494.27	0.48	DS/AM	1	2	5,277.18	5,922.05	10.89	DC/AR
4	0	2	-	3,590.02	3,586.65	3,586.65	0.09	FW	0	3	7,803.09	7,758.90	0.57	FW
5	1	2	-	5,944.02	5,922.05	5,922.05	0.37	DC/AR	1	3	8,550.16	9,077.84	5.81	DC/AR
6	-	-	3	5,961.23	6,652.4	5,898.96	1.06	DS/AM	2	2	9,787.95	10,084.17	2.94	DC/AR
7	0	3	-	7,791.15	7,758.9	7,758.9	0.42	FW	2	3	11,944.96	12,207.66	2.15	DC/AR

closed-closed cavity to its zero mode.

As a procedure to eliminate the modes of the structure in the coupled problem, the rigidity of the solid was increased, considering a higher elasticity modulus (fictitious) of $E = 2.1\times10^{15}$ N/m^2. For this value of E, the cavity behaves as if it had a rigid wall.

The modes that appear for standard E, which are not dominated by the cavity, are separated from the series and analyzed isolatedly. In any case, the modes suggest the influence of flexibility of the structure in the process of defining the origin (and/or prevalence) of the solid in the resulting modal signature.

It is also observed that the modes in the transverse direction ($n_x \neq 0$) do not nullify the effect of coupling, but allow the combination of coupled modes in (y) with the uncoupled cavity modes in (x).

4. Conclusions

When a higher elasticity modulus (E) is used, the dominant modes of the structure are eliminated and the values of natural frequencies of coupled cavity reproduce almost the same values of the uncoupled cavity case, but with slightly smaller magnitudes. However, the coupled one-dimensional modes (flat waves in y) are similar to those that appear in the uncoupled case, but with lower frequencies. Therefore, the difference between the analytical and numerical values is small, since the dominant modes of the structure are removed. Therefore, it is possible to evaluate coupled frequencies values.

These results present a good agreement for cases of reservoirs with a flexible bottom. Moreover, the frequencies and uncoupled numerical vibration modes of the structure were also compared with analytical solutions, showing satisfactory values.

Acknowledgments

The authors wish to thank the Brazilian National Counsel of Technological and Scientific Development (CNPQ) for material (equipment) and financial support (scholarships) provided during this research.

References

[1] O.C. Zienkiewicz, P. Bettess, Fluid-structure dynamic interaction and wave forces: An introduction to numerical treatment, International Journal Methods in Engineering 13 (1978) 1-16.

[2] E.L. Wilson, M. Khalvati, Finite elements for the dynamic analysis of fluid-solid systems, International Journal for Numerical Methods in Engineering 19 (1983) 1657-1668.

[3] O.C. Zienkiewicz, R.E. Newton, Coupled vibrations of a structure submerged in a compressible fluid, in: The Symposium on Finite Element Techniques, Stuttgart, 1969.

[4] W.J.T. Daniel, Performance of reduction methods for fluid-structure and acoustic eigenvalue problems, International Journal Methods in Engineering 15 (1980) 1585-1594.

[5] C.G. Everstine, Finite element formulations of structural acoustics problems, Computers & Structures 65 (3) (1997) 307-321.

[6] G. Sandberg, A new strategy for solving fluid-structure problems, International Journal Methods in Engineering 38 (1995) 357-370.

[7] G. Sandberg, P. Hansson, M. Gustavsson, Domain decomposition in acoustic and structure-acoustic analysis, Computer Methods in Applied Mechanics and Engineering 190 (2001) 2979-2988.

[8] L.C. Olson, K.J. Bathe, Analysis of fluid-structure interaction: A direct symmetric coupled formulation based on the fluid velocity potencial, Computers and Structures 21 (1-2) (1985) 21-32.

[9] L. Galli, R. Pavanello, Simplified finite element models applied to fluid-structure interaction problems, in: 8th Brazilian Symposium on Pipes and Pressure Vessels, Gramado, Brazil, 1994. (in Portuguese)

[10] L.J. Pedroso, Fluid-structure Interaction Course Notes, UnB-FT/ENC, Universidade de Brasilia, Brasília, 2003. (in Portuguese)

[11] X. Wang, On a mode superposition method for fluid-structure interaction problems, in: Proceeding of Symposium on Dynamics, Acoustics and Simulations, ASME IMCE, Anaheim, USA, Nov. 15-20, 1998.

[12] A.N. Barbosa, S.M. Souza, L.J. Pedroso, Sample of cases with fluid-structure coupling, in: XXXII South American Journey on Structural Engineering, Paper Code: JOR0568; Proceedings CD-ROM, Campinas, Brazil, 2006. (in Portuguese).

[13] S.M. Souza, A contribution to a fluid-structure coupled analysis methodology in acoustic cavities with flexible walls, Master Thesis, Civil and Environmental Engineering Department, University of Brasilia, Brazil, 2007, p. 177.

[14] L.C. Sousa, Applications of finite difference and finite element methods to fluid-structure interactions, Master Thesis, Civil and Environmental Engineering Department, University of Brasilia, Brazil, 2006, p. 197.

[15] ANSYS, Version 5.4, Swanson Analysis Systems, Inc., Houston, PA, 1997.